Cosmological Hydrodynamic Simulations of Preferential Accretion in the SMBH of Milky Way Size Galaxies

N. Nicole Sanchez [1,2]

Jillian M. Bellovary[1,2,3]

Kelly Holley-Bockelmann[1,2]

[1]Fisk University, Nashville, TN, USA, n.nicole.sanchez@vanderbilt.edu

[2]Vanderbilt University, Nashville, TN, USA

[3]American Museum of Natural History, New York, NY, USA

Received _____; accepted _____

Submitted to The Astrophysical Journal

ABSTRACT

Using cosmological hydrodynamic simulations of Milky Way-type (MW-type) Galaxies, we explore how varying assembly histories affect the mass budget of the SMBH. We examine two MW-mass halos with differing merger histories. One is characterized by several major mergers and the other with a quiescent history. We attempt to identify the importance of merger history on black hole accretion using varying resolution and SPH codes. This study is an extension of Bellovary et. al. 2013, which analyzed the accretion of high mass, high redshift galaxies and their central black holes, and found that the gas content of the central black hole is proportional to that accreted by the host galaxy halo. In this study, we find that a merger-rich galaxy will have a central SMBH preferentially fed by the merger gas fueling the system. A quiescent galaxy, however, will have a SMBH that mirrors its host's composition. Through an investigation of the angular momentum of the gas entering these hosts and their SMBHs, we determine that merger gas enters the galaxy with lower angular momentum compared to smooth accretion, partially accounting for the preferential fueling witnessed in the SMBH of the galaxy with an active merger history. In addition, the presence of mergers, particularly major mergers (q >0.3), also helps funnel the low angular momentum gas more readily to the center of the galaxy. Our results imply that galaxy mergers play an important role in the feeding of the SMBHs in the class of Milky Way-type galaxies.

Subject headings: Black hole physics – Galaxies: spiral – Galaxies: kinematics and dynamics – Methods: Numerical – Others

1. Introduction

Supermassive black holes (SMBHs) are thought to exist in almost all massive galaxies (Kormendy & Ho 2013). In the canonical picture of BH growth, these black holes may become active galactic nuclei (AGN) during periods of high accretion and wane in periods of quiescence (Alexander et al. 2005; Papovich et al. 2006; Volonteri 2012). The host galaxy's size, star formation rate, and other environmental effects may help to influence the growth of the black hole residing at its center; however, there are still uncertainties concerning the relationship between these SMBHs and their much larger host galaxies, as well as how they grow and evolve together (Haehnelt & Kauffmann 2000; Di Matteo et al. 2005; Hopkins et al. 2006; Fu & Stockton 2008; Sijacki et al. 2009; Silverman et al. 2009; Mullaney et al. 2012).

The M$-\sigma$ relation, which relates the SMBH's mass and the velocity dispersion of the host galaxy's central stellar population, gives some insight into the complex interplay between these objects (Ferrarese & Merritt 2000). A prominent trend appears, as SMBHs tend to scale with the velocity dispersion of the host galaxy bulge. The tightness of the relation is significant and can be seen over several orders of magnitudes in velocity dispersion and black hole mass (Merritt & Ferrarese 2001b; Graham et al. 2011; Mcconnell & Ma 2013; Kormendy & Ho 2013). Scatter exists among the low mass galaxies and a deviation may appear at the high mass end, where overmassive BHs may reside (Van Den Bosch et al. 2007; Moster et al. 2010; Natarajan 2011). However, scatter in less massive galaxies may imply that there are several channels of black hole growth at play in the low mass end of the relation (Micic et al. 2007; Volonteri & Natarajan 2009; Reines et al. 2013; Graham & Scott 2014). One standard explanation for the M$-\sigma$ relation lies in galaxy mergers, which build up galaxies, feed SMBHs, and assemble bulges (Di Matteo et al. 2005; Shen et al. 2008). Major mergers are thought to supply gas to the central SMBH resulting

in feedback which quenches star formation and affects the structure of the galaxy.

The black hole mass-bulge luminosity relation was implied by the work of Dressler & Richstone (1988) and first illustrated by Kormendy (1993). A wealth of evidence continues to relate these two characteristics, and follow up examinations using HST observations have determined the current, best estimates yield a M_{BH}/M_{bulge} fraction between about 0.0013 and 0.0023 (Merritt & Ferrarese 2001a; McLure & Dunlop 2001; Marconi & Hunt 2003).

Major mergers between massive galaxies are thought to be efficient fueling mechanisms for bright AGN. The large influx of material due to tidal torques from the merger causes bursts of star formation and helps funnel gas directly into the center where the SMBH resides (e.g. Richards et al. 2006; Reddy et al. 2008; Hopkins & Quataert 2010). Additionally, the most massive, highest-luminosity AGN (i.e. quasars) reside in incredibly luminous infrared galaxies where star formation is abundant, signifying that major mergers may have recently occurred (Treister et al. 2012). Distorted morphologies are often characteristics of quasar hosts, and companions can also be present around quasars, both of which are evidence that strengthen the possibility of a recent merger having affected their lifetimes.

In many less massive and less luminous AGN, however, there is a clear lack of distorted morphologies, close neighbors, and/or other obvious merger evidence (Ryan et al. 2007; Schawinski et al. 2011; Ellison et al. 2013; Hicks et al. 2013). It is also important to note that many of these AGN exist in spiral galaxies, which are unlikely to have been recently disturbed by major mergers (Springel & Hernquist 2005; Kocevski et al. 2011). Nevertheless, some evidence suggests (van Gorkom & Schiminovich 1997; Governato et al. 2009b) that disturbed galaxies may reform a disk quickly, even after a major merger as long as it is gas-rich. More recently, Treister et al. (2012) has suggested that only the highest luminosity AGN require fueling via major mergers; ∼90% of AGN across all redshifts are fueled by various other mechanisms which may include minor mergers, flybys, and smooth

accretion, whereby gas is directly accreted via large filaments from the ambient intergalactic medium (Cox et al. 2006; Bellovary et al. 2013; Sinha & Holley-Bockelmann 2012).

Smooth accretion, in particular, may play an important role in fueling these low mass galaxies. Halos less than 10^{11} $M_{\odot}$ can accrete filaments of unshocked gas; thereafter, gas will shock heat to the virial temperature of the halo (Keres et al. 2005). Even for massive halos, unshocked gas may still penetrate shocked regions to fuel the galaxy (Brooks et al. 2007; Dekel et al. 2009; Nelson et al. 2013). In addition, SMBH feedback, the depositing of energy and angular momentum back into the gas resevoir during accretion, also affects the overarching structure of the host galaxy (Governato et al. 2009a). Secular processes, including bar formation and disk instabilities, may also be prominent forms of accretion for these SMBHs (Kormendy & Ho 2013).

It is clear that galaxy hosts grow through a variety of channels that depend on mass, environment, and interaction history. Therefore, we want to understand how these different galaxy evolutionary paths translate into SMBH fueling mechanisms, and see how they affect the fueling gas flowing into the SMBH itself. Bellovary et al. (2013) compared simulations of three high mass, high redshift galaxies and found that while mergers and smooth accretion both efficiently build up galaxies, no particular method was more adept at feeding the SMBH. Using a similar method as Bellovary et al. (2013), this work compares the SMBH and galaxy fueling mechanisms between two Milky Way (MW) mass galaxies. MW-type galaxies host SMBHs on the order of 10^{6} $M_{\odot}$, which are likely the most common type of massive black hole, yet little is known about them or how they may grow (Kormendy & Ho 2013). Through this examination, we hope to better understand the coevolution of SMBHs and their hosts in this class of galaxy.

We analyze two galaxy simulations that are similar at z = 0 but have very different merger histories. Our "active" galaxy, h258 (Figure 1), has a history characterized by

major mergers, while our "quiet" galaxy, h277 (Figure 2), has a quiescent history with only minor mergers. Since these galaxies are similar to the MW in virial mass, stellar mass, and circular velocity, without a deeper examination, we may not recognize the varying histories that distinguish them. We will compare the origins of gas entering the SMBH and halo to look for clues about SMBH fueling within these galaxies. By examining the assembly of these galaxies, and their SMBH fueling, we compare the accretion rates between h258 and h277 to determine how SMBHs grow in galaxies like our own.

2. Simulation Parameters

The cosmological simulations have been run using two smoothed particle hydrodynamics (SPH) N-body tree code: Gasoline (Wadsley et al. 2003) and, more recently, Charm N-body GrAvity solver, ChaNGa.

An initial DM-only, uniform resolution 50 comoving Mpc box determined which halos would be selected for zoom-in examination, including the two halos examined in this paper. The DM-only simulation assumed a WMAP Year 3 cosmology (Spergel et al. 2007) with the following specifications: $\Omega_m = 0.24$, $\Omega_\Lambda = 0.76$, $H_0 = 73$ km/s, and $\sigma_8 = 0.77$. The halos h258 and h277 were chosen for their Milky Way-mass, between 6–8 $\times$ 10^{11} $M_\odot$, at z=0 and their active and quiescent merger histories, respectively. The halos have virial masses defined relative to a critical density, ρ_c, where $\rho/\rho_c = 100$ where h258 and h277 have virial masses of $M_{\rm vir} = 7 \times 10^{11} M_\odot$ and $M_{\rm vir} = 8 \times 10^{11} M_\odot$, respectively. A recent major merger characterizes the h258 halo at z=1, while h277 has its last significant merger near z $\sim$ 3. A second "zoom-in" high resolution simulation was run for both of these galaxies including gas and star particles using the volume renormalization of Katz & White (1993), resimulating only a few virial radii from the main halo at the highest resolution. The Gasoline and ChaNGA simulations were run from z=99 to z=0 and z=150 to z=0, respectively.

Gas can reach a minimum temperature of ∼100 K, in the absence of cooling via molecular hydrogen or metals. The simulation includes stochastically-modeled star formation, and once the density threshold and temperature satisfy conditions for star formation (1.0 and 10.0 amu cm^{-3} for Gasoline and ChaNGa, respectively; T $<10^4$ K, for both simulations), gas particles are eligible to form stars with an efficiency of c* = 0.1. Star particles form along the Kroupa initial mass function (Kroupa 2001). Supernova feedback releases 10^{51} ergs of thermal energy and affects a "blastwave" radius determined by the equations of Ostriker & McKee (1988). In the affected region, cooling turns off for a time relative to the expansion phase of the SN remnant also determined by the blastwave equation. SN Ia and II from Thielemann et al. (1986) and Woosley & Weaver (1986) are adopted, respectively, and implemented through the Raiteri et al. (1996) method, which uses the stellar lifetime calculations of the Padova group (Alongi et al. 1993; Bressan et al. 1993; Bertelli et al. 1994) to describe stars with varying metallicities. Both the supernova "blastwave" radius and supernova (Ia and II) prescriptions are described in detail by Stinson et al. (2006). A low-temperature extension to the cooling curve is used to trace metals (Bromm et al. 2001). Simulated galaxies are shown to conform with the observed Tully-Fisher relation (Governato et al. 2009b), the size-luminosity relation (Brooks et al. 2011), and the mass-metallicity relation (Brooks et al. 2007), in addition to having realistic matter distributions and baryon fractions (Governato et al. 2009a; Guedes et al. 2011). Parameter and resolution choices described above allow the galaxies to adhere to the stellar-mass-halo-mass relation at z=0 and maintain a realistic period of star formation (Moster et al. 2010; Munshi et al. 2013; Brooks et al. 2007; Maiolino et al. 2008). Given the strict adherence of these simulated galaxies with observations, we are confident that they reasonably represent growth in the galaxy and its SMBH. We exclude AGN feedback in these small to moderate mass-galaxies; however, we have determined that has little effect on the global properties of the galaxy and SMBH.

Since there are uncertainties in the formation of black holes "seeds," we implement a BH seeding method that is broadly consistent with several theories of direct collapse black holes (Couchman & Rees 1986; Abel 2002; Bromm & Larson 2004) and Population III stellar remnants (Loeb & Rasio 1994; Eisenstein & Loeb 1995; Koushiappas et al. 2004; Begelman et al. 2006; Lodato & Natarajan 2006). While this method allows the BH formation process to remain physically motivated, BH seeds form if their parent gas particle matches the criteria required for star formation and also maintains zero metallicity (2.5 amu cm^{-3}; T $<10^4$ K; Z = 0) (Stinson et al. 2006). A probability of $\chi_{seed} \sim 0.01$ is applied to determine whether a gas particle (with the above specifications) will become a BH seed with a mass of $M_{BH} = 2.28 \times 10^5$ $M_\odot$, the same mass as its parent gas particle. This probability was chosen to match the predicted occupation fraction of BH seeds at z $\sim$ 3 (Volonteri et al. 2008).

The requirement that BH seeds must form from zero metallicity gas particles also causes BH formation to be constrained in areas of early star formation bursts, where the earliest and most massive halos are expected to form in the simulation. BH formation is dependent only on local environment, neglecting any large-scale properties of the host halo. Black holes are not fixed within the center of their host, allowing them to be dynamically affected by mergers and other perturbations within the galaxy. Nevertheless, BHs remain near their host centers by choosing dark matter particle masses in high-resolution regions to be on the same order as gas particle masses, minimizing two-body interactions (Bellovary et al. 2011).

Black hole mergers occur when they are separated by less than twice the softening length, and must be bound or satisfy $(1/2)\delta v^2 < \delta a \cdot \delta r$, where δv and δa are the velocity and acceleration differences between the two black holes and δr is the distance separating them. In addition to gaining mass via merger, black holes gain mass through Bondi-Hoyle

gas accretion:

$$\dot{M} = \frac{4\pi\alpha G^2 M_{\rm BH}^2 \rho}{(c_s^2 + v^2)^{3/2}}, \quad (1)$$

where α is a constant equal to 1, ρ is the density of the surrounding gas, c_s is the sound speed, and v is the black hole's relative velocity to the gas. Feedback is applied to surrounding gas with an energy boost determined by the accreted mass as follows: $\dot{E} = \epsilon_r \epsilon_f \dot{M} c^2$ where $\dot{M}$ is the accreted mass, and $\epsilon_r = 0.1$ and $\epsilon_f = 0.03$ are assumed for the radiative efficiency and feedback efficiency, respectively. This energy is distributed as thermal energy to the 32 nearest particles via a kernal probability function. Though other groups use a higher value for this efficiency, $\epsilon_f = 0.05$ (Sijacki et al. 2007; Di Matteo et al. 2008), we find that $\epsilon_f = 0.03$ in our code produces MBHs in better agreement with MBH-host galaxy scaling relations. However, as our main concern is in the relative proportion of gas in various phases, our results are not sensitive to our choices of ϵ_r or ϵ_f.

2.1. Low Resolution GASOLINE Simulations

Our low resolution simulations were run using the smoothed particle hydrodynamics (SPH) N-body tree code Gasoline (Wadsley et al. 2003), with a force resolution of 320 pc and the gas, dark matter, and star particle masses of 2×10^5 $M_\odot$, 3×10^5 $M_\odot$, and 7×10^4 $M_\odot$, respectively. Both N-body+SPH volume renormalized simulations of h258 and h277 have been previously examined in other publications. For example, Governato et al. (2009b) studied the regrowth of the large disk structure in h258 after its major merger.

2.2. High Resolution CHANGA Simulations

To determine whether our results are biased due to low resolution, we created a high resolution version of h258 with the following properties: a spline force softening length

of 174 pc and initial gas particle masses of $2.7 \times 10^4 M_\odot$. Star particles are created with 30% of their parent gas particle mass, allowing a maximum initial mass of 8100 $M_\odot$. Each galaxy contains about 5 million DM particles inside the virial radius at z=0 and over 14 million DM, star, and gas particles total. The resolution of both force and mass in these simulations is comparable to the "Eris" simulation which has one of the highest resolutions for an N-body+SPH cosmological simulation of a Milky Way-mass galaxy so far produced. At z=9, a uniform UV background is applied to simulate the cosmic reionization energy in a variation of Haardt & Madau (2012).

This volume was run using Charm N-body GrAvity solver, ChaNGa, which scales better and includes a new improved SPH formalism (Keller et al. 2014). The hydrodynamic treatment now includes a geometric density average—$(P_i + P_j)/(\rho_i \rho_j)$ rather than $P_i/\rho_i^2 + P_j/\rho_j^2$ where P_i and ρ_i are the particle's pressure and density—in the force expression, in addition to the standard SPH density estimator (Ritchie & Thomas 2001). Adjusting the force expression diminishes tensions in the numerical surface due to shear flows, such as Kelvin-Helmholtz instabilities. We also apply a consistent and entropy-conserving energy equation to account for the modified force expression and correctly model strong shocks, such as Sedov blasts.

3. Reduction Method

The Amiga Halo Finder identifies and sets the virial radii in a simulation using an overdensity criterion for a flat universe (Knebe et al. 2001; Knollmann & Knebe 2009; Gill et al. 2004). We select the primary halo to be the most massive galaxy at z=0 and locate the central SMBH. For our Gasoline simulations, both the primary halo in h258 and h277 had final masses on the order of $10^{12} M_\odot$ and a formation redshift of z$\sim$4.

In this analysis, we retrace each gas particle that was accreted by the galaxy or SMBH, following the gas back through its journey in the galaxy and recording its host halo and time of accretion (Brooks et al. 2009). The particles are then classified into types by their method of entrance into the primary halo. In particular, gas particles that exist in the primary halo at the first time step are classified as "early" gas. Gas that belonged to a different halo than the primary prior to accretion is classified as "clumpy," entering the primary halo through mergers. All other gas is classified as "smooth" accretion, and is then subdivided into two categories: "cold" and "shocked." Cold or unshocked gas will usually flow into the halo via large-scale, dark matter filaments (Bellovary et al. 2013). It's possible for cold gas to be dense enough to pierce an already developed shock, allowing it to funnel into the galaxy core where it can be accreted onto the SMBH.

However, as we discussed in Section 1, if the galaxy halo is $\gtrsim 10^{11}$ $M_\odot$, the gas is known to shock heat up to the virial temperature of the halo. We identify shocked particles through an increase in entropy and temperature using the following criteria:

$$T_{\rm shock} \geq 3/8 T_{\rm vir}, \tag{2}$$

where $T_{\rm vir}$ is the virial temperature of the halo and $T_{\rm shock}$ is the temperature of the gas particle, and

$$\Delta S \geq S_{\rm shock} - S_0, \tag{3}$$

where S_0 is the initial entropy of the gas particle, and

$$S_{\rm shock} = log_{10}[3/8 T_{\rm vir}^{1.5}/4\rho_0], \tag{4}$$

where ρ_0 is the gas density prior to the shock. Since our halos are $\sim 10^{12}$ $M_\odot$ by z = 0, we should expect to find more shocked gas entering the halo.

Once all the gas particles have been individually categorized, we can use these labels to determine which particles are accreting onto the SMBH, and we can better contrast the

methods that feed the galaxy and its SMBH in MW-mass halos.

4. Results

From the initial analysis of the low resolution Gasoline simulations, we have determined that the merger histories of these two galaxies has a pronounced effect on the resulting accretion of gas into the SMBH and its host.

4.1. Gasoline - Low Resolution h258: Resolution Test

The galaxy h258 is characterized by an active merger history, including a major merger (q=0.9, with an incoming gas mass of 1.26×10^{10} $M_{\odot}$) at z=1 (Figure 1). The merger can be seen increasing the cumulative black hole mass (Figure 3) as well as the gas fractions within both the SMBH and galaxy (Figure 4). Figure 3 shows the cumulative SMBH mass in h258 as a function of time (lower axis) and redshift (upper axis). The black dashed line indicates the total cumulative BH mass (including both mass from gas and BH mergers), while the black solid line indicates the total accreted gas mass. The blue dot-dashed line represents the gas mass accreted via unshocked gas, while the green solid line and red dashed line show the gas mass accreted through mergers and shocked gas, respectively. It is also worthwhile to point out that the largest part of the mass budget at high redshift is not gas at all, but other black holes that have merged with the SMBH seed. This has important implications for gravitational wave astronomy, increasing the event rate for SMBH assembly at high redshifts (Holley-Bockelmann et al. 2010). Aside from this early BH assembly, the largest gain in SMBH mass comes from gas associated with the major merger at z $\sim$ 1. Figure 4 shows the fractions of unshocked and clumpy gas compared to all accreted gas as a function of redshift. It confirms that unshocked gas makes up the majority of gas entering

the galaxy at early times. Nevertheless, around the time of the merger (z $\sim$ 1) a marked change occurs in the gas fractions and clumpy gas becomes the main component of total gas in the BH.

Figure 5 depicts the fractions of total gas in the galaxy (a) and the SMBH (b) at z=0, again differentiated by gas origin. Blue, green, and red distinguish cold, clumpy, and shocked, respectively. Yellow indicates gas that existed within the main halo upon formation. The galaxy has a mass nearly half comprised of gas entering the galaxy through unshocked, smooth accretion (48 %), with 39 % of the gas entering through mergers. The smallest fractions of the total gas are comprised of shocked gas (9 %) and "early"gas that existed at formation makes up the final, smallest fraction (4 %). Unlike the galaxy, nearly 65 % of the gas accreted by the central SMBH was gas accreted via mergers, while only a quarter (26 %) is comprised of unshocked, smoothly accreted gas. Shocked gas makes up the last 9 % of total gas entering the SMBH, along with a negligible ($<$ 1%) amount of "early" gas. **It is evident then that the SMBH more readily accretes gas gained through mergers.** This result is contrary to Bellovary et al. (2013) which found that the fractions of gas comprising the SMBH and its host were nearly the same. Through our results, we find that lower mass galaxies can readily employ the physical effects of mergers to feed their SMBH.

To better understand the apparent preference for merger-accreted gas, we examine the angular momentum of each type of gas at the moment it enters the galaxy. Figure 6 shows that gas entering the SMBH (dashed lines) has an overall lower angular momentum than gas entering galaxy (solid lines), as expected; this statement is true regardless of the gas state.

Figure 7 explicitly shows that at the time of the merger, the lowest angular momentum gas entering the galaxy (solid lines) is merger-driven (green, solid line). This is reflected in

the SMBH (green, dashed line) as nearly all the clumpy gas at this time funnels directly into the SMBH.

NOTE: *Need to add a figure that clearly supports this argument. Possibly a series of angular momentum plots at the times of mergers. Or comparisons between cumulative distributions at time with and without mergers.*

4.2. Gasoline - Low Resolution h277: Resolution Test

Our quiescent galaxy, h277, was characterized by few mergers in its past, its final major merger occuring around z $\sim$ 3 (Figure 2). This merger is visible in Figure 8, though more subtle than the influx of gas in h258. (Linestyles as in Figure 3.) In h277, gas seemed to be gained at a more steady rate and at fairly high redshifts comprises a larger portion of the BH's total mass than seen in the previous, more active galaxy. The gas fractions (Figure 9) in h277 (solid lines) and SMBH (dashed lines) are also markedly different than that of a galaxy with an active merger history. While it appears neither clumpy or unshocked gas (green and blue, respectively) particularly dominates at higher redshifts in the galaxy, merger gas becomes prominent in the SMBH at times when mergers occur. [**Ref merger tree when included.**] Again, this implies some physical process allowing merger gas to readily fuel black hole growth. Though, it is important to note that by z $\sim$ 0, smoothly accreted, unshocked gas again dominates in both the SMBH and host galaxy. As in our more active galaxy, it appears that the role of clumpy gas as it fuels the SMBH becomes important when mergers affect the galaxy; however, with h277 having a significantly less active merger history, unshocked, smooth accretion inevitably dominates the total gas supply.

This result can be more clearly seen in Figure 10. (Colors as in 5.) Similar to Bellovary

et. al. 2013 study, which found SMBH accretion in high mass, high redshift galaxies mirror their hosts in terms of accreted gas, h277's SMBH accretes a similar fraction of each type of gas, comparable to its host galaxy. Smoothly accreted, unshocked gas represents about half of the total gas in both the SMBH and the galaxy. Clumpy gas also maintains about 30% of both, while an increase in shocked gas occurs, from 13% in the galaxy to 22% in the SMBH. So by present day, h277 found no strong preference for the SMBH to prefer any one kind of gas in its accretion. Like the SMBHs in the study of Bellovary et al. (2013), nearly the same fractions of gas entering the halo would then be accreted onto the SMBH (with the exception of shocked gas). Therefore, this may imply that without some physical driver, like the major merger of h258, clumpy gas is unlikely to dominate the gas accreted into the SMBH.

As in the previous case, we examined the angular momentum of all the gas particles accreted by the SMBH and host galaxy at the moment of entry. (Figure 11; Linestyles as in 6) Like before, it is immediately apparent that the clumpy gas accreted by both the black hole and its host has a lower angular momentum overall than the smoothly accreted gas; however, unlike we found in h258, the h277 galaxy accretes gas with lower angular momentum than that of its SMBH. This appears to imply that some of the gas with the lowest angular momentum is remaining in the host galaxy rather than accreting onto the SMBH.

As h277 and h258 are similar in size and appearance at z=0, these differences indicate that the varying histories of these simulations appears to play an important role in the evolution of these types of galaxies and their central SMBHs. We also note that while mergers may not be the only physical mechanisms by which gas can be funneled into the centers of galaxies, mergers between galaxies clearly play an important role when considering the gas accretion of SMBHs.

4.3. ChaNGa - High Resolution h258

Just as we found in the same galaxy, h258, of the lower resolution simulation, the high resolution h258 galaxy sees a distinct preference for accreting gas that has been gained through the many mergers in its history. In this version, h258 is characterized by two major mergers; the first occurs at z $\sim$ 1.8 and the second at z $\sim$ 1.2. Unlike its predecessor, this h258 has a smoother history of overall gas accretion (Figure 12; Linestyles as in Figure 3). However, the transitions between when smooth, unshocked accretion and mergers dominate is clearly distinguished. While clumpy gas (green) dominates at the earliest time, unshocked gas (blue) overtakes it for a short time ($\sim$ 2 Gyr) before clumpy gas once again dominates by z $\sim$ 1.5.

This low redshift transition to a clumpy gas preference results in the large fraction of clumpy gas seen in the SMBH (Figure 13; Colors as in Figure 5). We can see from the figure that comparable to the Gasoline h258 version, the amount of unshocked, cold gas in the SMBH (24%) is less than that entering the galaxy (36%). The shocked gas, however, sees a sharper decline in the amount of shocked gas that enters the SMBH ($\sim$2%) than in the host (8%). This differs from the Gasoline h258 results and may be attributed to the higher resolution of the second iteration. Figure 13 also explicitly shows how the fraction of clumpy gas accreted by the SMBH (74%) is significantly larger than the fraction of clumpy gas accreted by the host galaxy (56%). **This result, which repeats the analysis with an improved and higher resolution simulation, confirms the initial study's findings!** This confirmation makes us confident that these results are well founded.

In keeping with the analysis of the Gasoline galaxies, we followed up the study of the galaxy and SMBH gas fractions by examining the angular momentum of the accreted gas particles. Figure 14 (Colors as in Figure 6.) shows a cumulative distribution of the gas particles' angular momentum as they enter the halo, distinguished between gas that ends up

in the SMBH (dashed line) or the galaxy (solid lines) at z=0. This plot is consistent with Figure 6, as the angular momentum of gas entering the SMBH is lower when comparing between types of gas. In the ChaNGA h258 case, however, we see that the lowest angular momentum gas is comprised of both clumpy and unshocked gas, unlike in the Gasoline version which clearly showed that unshocked gas entered the SMBH with the lowest angular momentum. We attribute this variation to the subtle difference between the histories of the two simulations, including the two mergers which characterize the higher resolution version. This can be seen if we examine Figure 15 which shows the cumulative distribution of the angular momentum of the incoming gas particles at the time of the second merger. (Colors and linestyles as in Figure 7.) Figure 15 explicitly shows that the gas ending up in the SMBH enters with the lowest angular momentum. This result is similar to what we found in the Gasoline h258 simulation, however, in the previous case it appeared that all the low angular momentum gas entering at the merger timestep ended up in the galaxy. Yet the distinction remains as there appears to be an influx of gas with low angular momentum feeding the black hole at this timestep that is not associated with the merger occurring at z $\sim$ 1.2. This may be attributed to the prior merger at z $\sim$ 1.8 (Figure 16) during and after which a large influx of low angular momentum gas enters the galaxy and SMBH. (Color and linestyles as in Figure 15)

5. Conclusion

This study examines the gas accretion onto two fully cosmological simulations of Milky Way-size galaxies to redshift z = 0, one with a quiescent merger history and one with major mergers characterizing its past. A second iteration of the latter, simulated with higher resolution and improved physics, is also examined. In each case, we trace the gas into the SMBHs at their centers and differentiate the gas accreted onto the galaxy and SMBHs by

origin. Gas gained through mergers is classified as "clumpy" gas and smoothly accreted gas is seperated into "shocked" and "unshocked" categories. Our goal is to determine what types of gas are primarily feeding the SMBH and the galaxies of this class, and to determine what effects the merger histories of the galaxies may have on these processes.

When we examine the accretion of the galaxy with a quiescent history, we note that smooth accretion is the dominant feeding mechanism for both the galaxy and its central SMBH. We find that the fractions of each type of gas comprising the overall mass of the SMBH are comparable to the fractions of the gases making up its host. This result is consistent with the results of Bellovary et al. (2013) which similarly analyzed high mass, high redshift galaxies and found the gas composition of the SMBHs mirror their host.

Contrary to these previous results, when we examined the galaxy with an active merger history, we determined that the SMBH at the center more readily accretes gas gained through mergers. **In both the low and high resolution cases, we see a significant increase in the clumpy gas accreted by the SMBH compared to its host.**

The angular momentum of the accreted gas as it enters the galaxy sheds some light on the mechanism driving this preferentially accreted clumpy gas. Smoothly accreted gas, which enters with galaxy with a wide range of angular momentum, may become additionally torqued by the already existing disk. Meanwhile, gas entering through mergers is restricted by the direction of its entry and allows for a small range of low angular momentum gas to enter the main halo. This gives clumpy gas the advantage of falling more readily to the center and accreting onto the SMBH. Considering all origins of gas, we see a clear distinction wherein lower angular momentum gas preferentially feeds the SMBH.

This however, does not remain true when we look again at the galaxy with a quiescent history. In this case, some of the gas entering the galaxy with the lowest angular momentum remains outside of the SMBH. This results implies that some of the physical processes

affecting the galaxy with an active merger history accounts for the ready funneling of low angular momentum to the central region of the black hole.

While the examination of these two extreme cases of galaxy merger history depict a class of galaxy with varying SMBH accretion methods, a further study of intermediate cases is required to begin understanding the broad spectrum of Milky Way-mass galaxy accretion. It is clear through this study that the presence (or absence) of major mergers can play an important role in the final compositions of central SMBHs, but the question of how important these mergers are remains to be seen.

Thank you to the Fisk-Vanderbilt Masters-to-PhD Bridge program for their continued funding and support of this research. Also thank: American Museum of Natural History. N-Body shop, for use of their code? Others? [GET GRANT NUMBERS?]

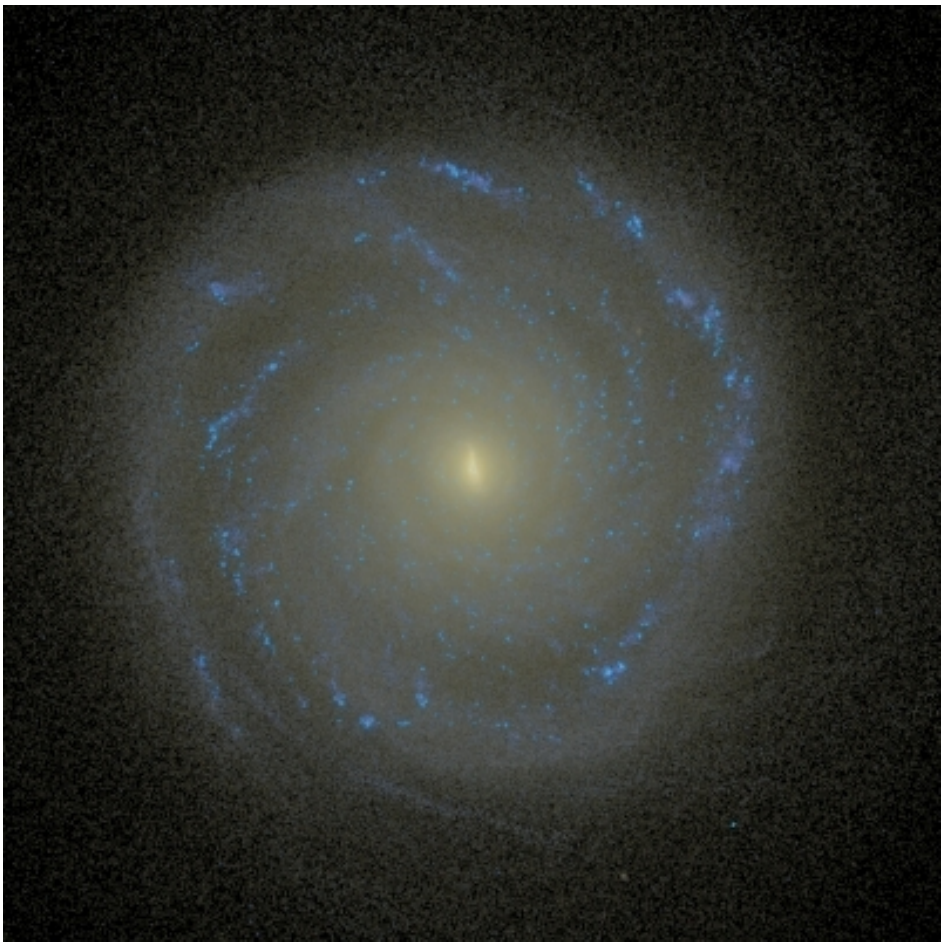

Fig. 1.— Face-on and edge-on Sunrise images of our GASOLINE galaxy, h258, which has an active, merger-rich history.

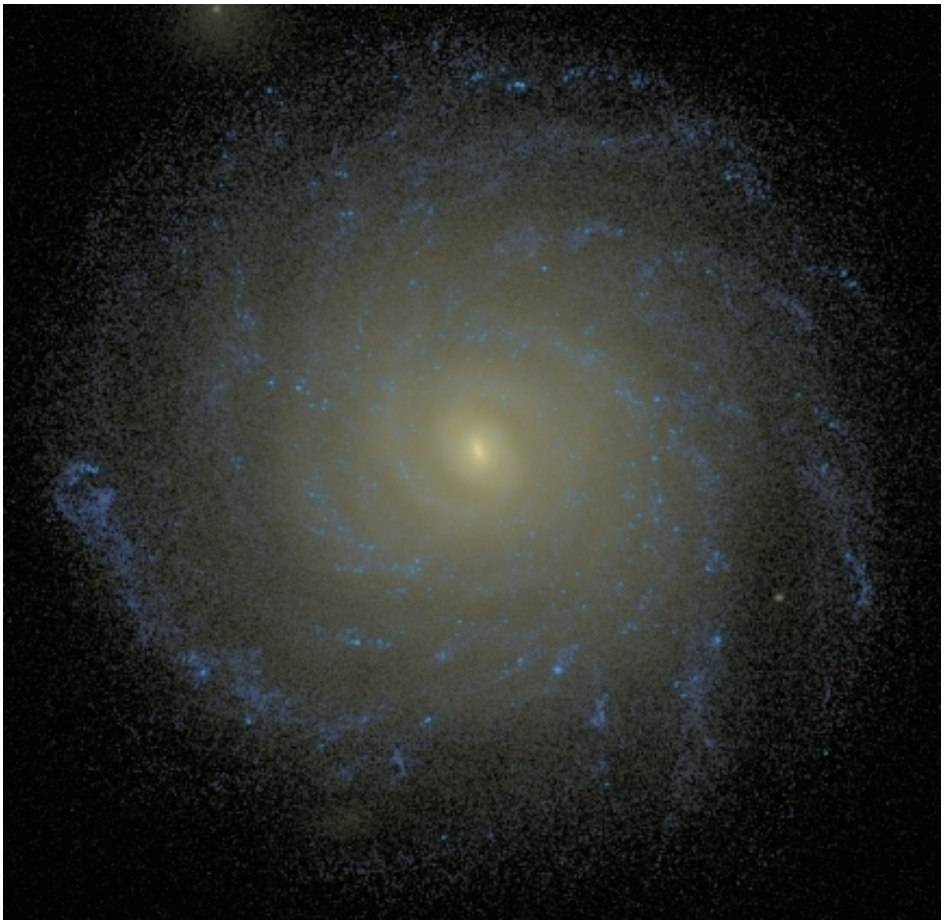

Fig. 2.— Face-on and edge-on Sunrise images of our GASOLINE galaxy, h277, which has a quiescent, merger-quiet history.

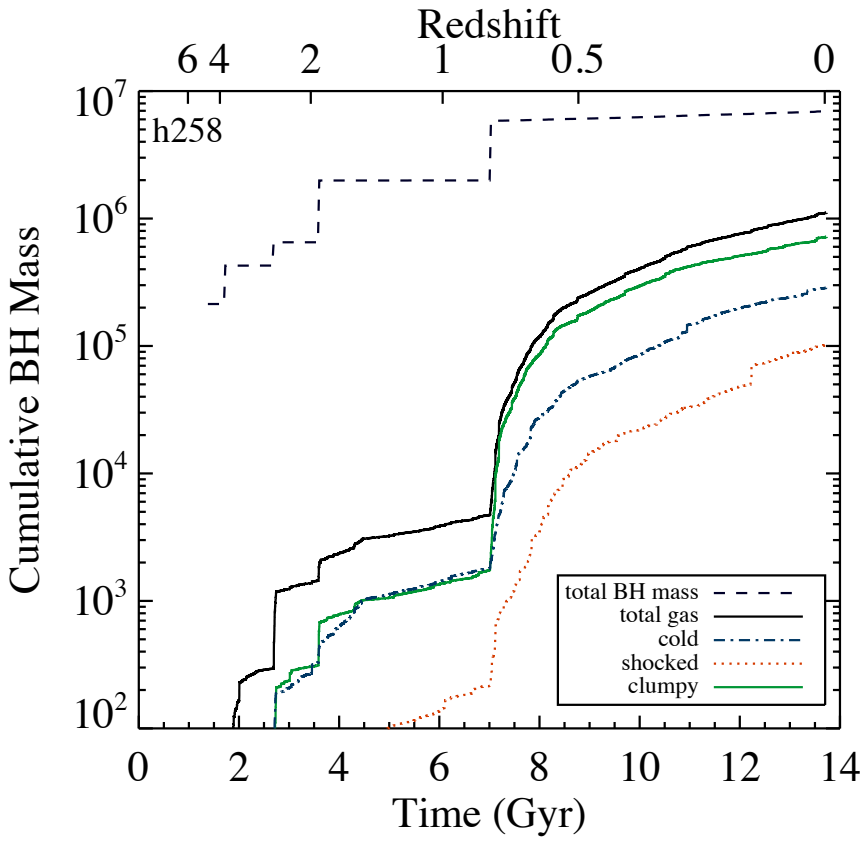

Fig. 3.— The central BHs cumulative mass as a function of time and redshift. The black dashed line indicates the total cumulative BH mass. The black solid line indicates the total gas mass. The blue dot-dashed line indicates the gas mass accreted via unshocked gas. The green solid line indicates the gas mass accreted through mergers. The red dashed line indicates gas mass that was shocked upon entry into the halo.

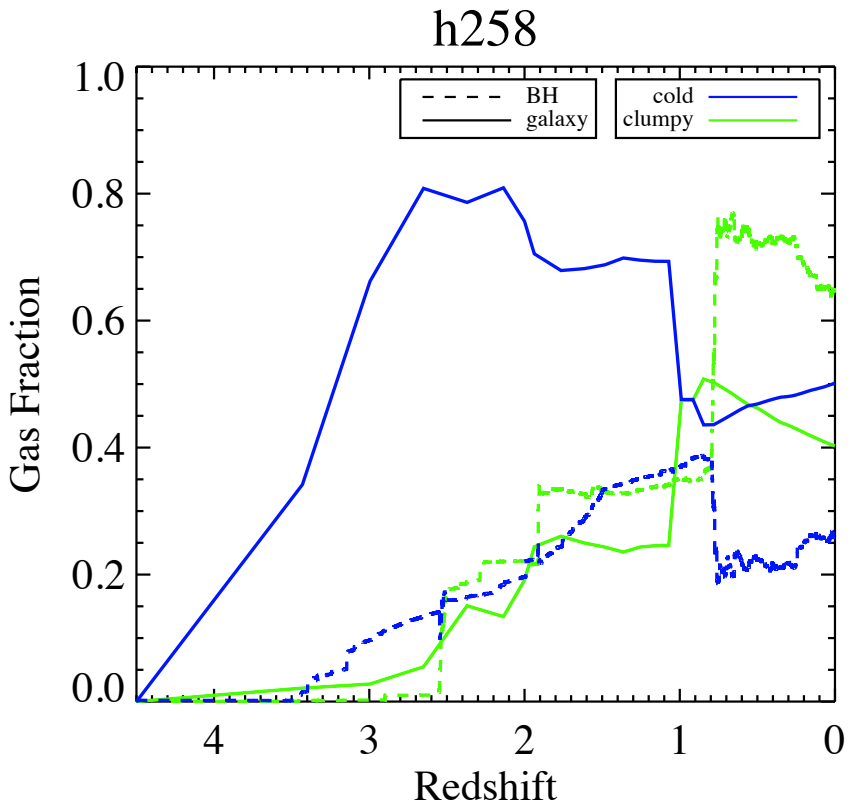

Fig. 4.— Gas fraction across redshift for galaxy (solid lines) and central BH (dashed lines). Green lines signify gas fractions accreted via mergers and blue lines designate gas accreted via unshocked gas filaments.

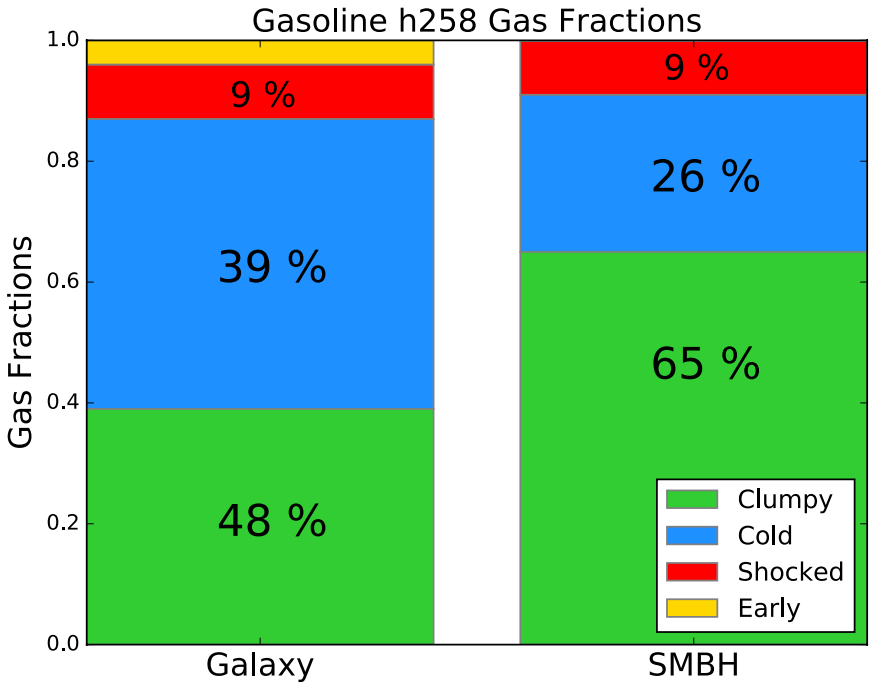

Fig. 5.— Gas fractions of the gas particles accreted in h258 by the main halo (left) and the SMBH (right), distinguished by type. Blue, green, and red distinguish gas gained through unshocked gas, gained through mergers, and gas shocked upon entry, respectively. Yellow indicates gas that existed within the main halo upon formation; this "early" gas is negligible (< 1 %) within the SMBH.

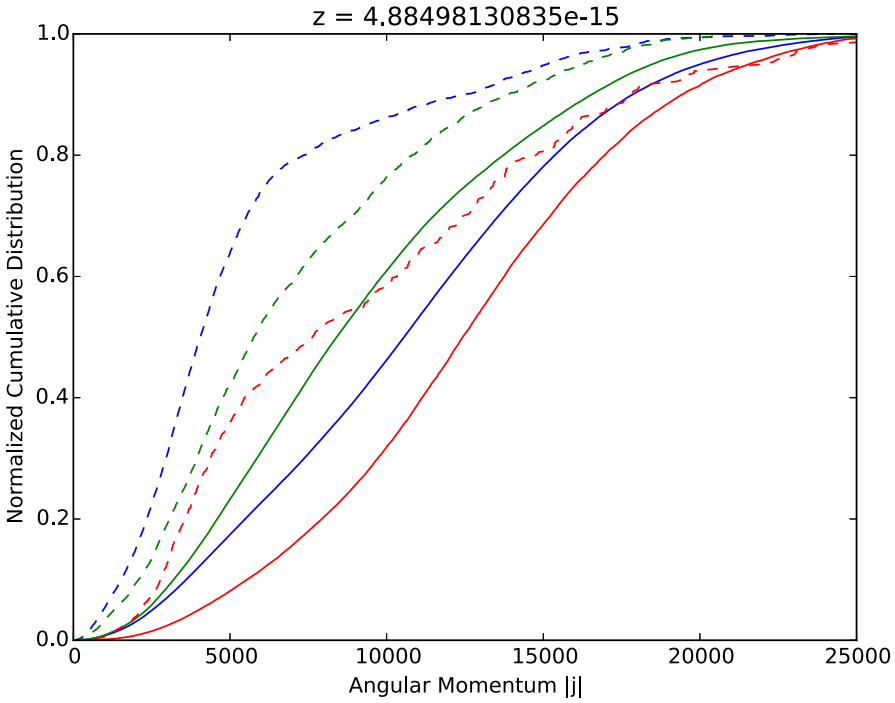

Fig. 6.— Cumulative distribution of angular momentum of the gas particles accreted onto h258. Gas particles accreted onto the main halo (solid lines) and central black hole (dashed lines). The green, blue, and red lines indicate clumpy, unshocked, and shocked gas, respectively.

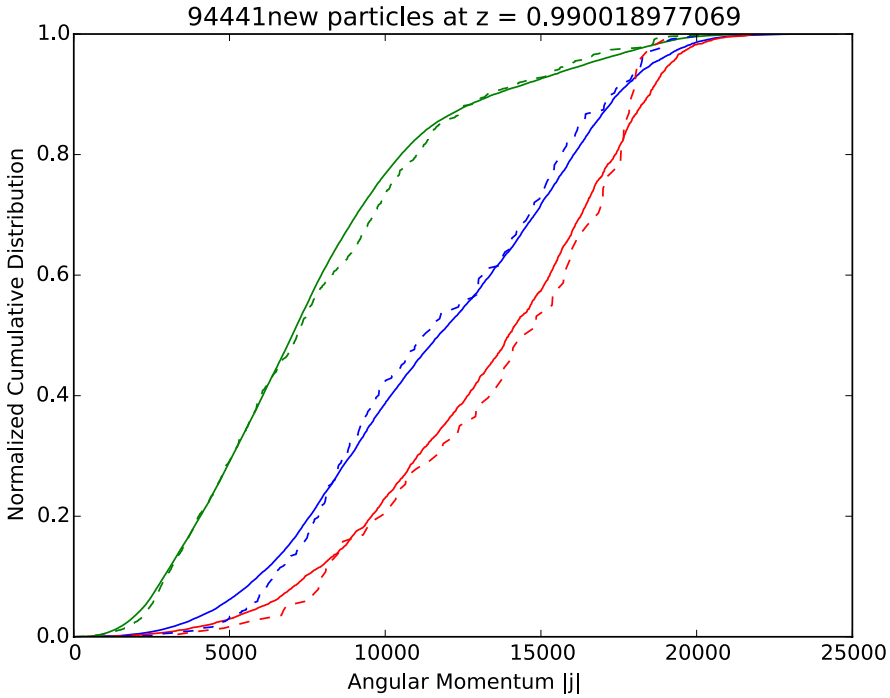

Fig. 7.— Cumulative distribution of angular momentum of the gas particles accreted onto h258 at the time of the major merger (z $\sim$ 1). There are about 95,000 gas particles accreted at this timestep, which gas particles accreted onto the main halo and central black hole distinguished by solid and dashed lines. The green, blue, and red lines indicate clumpy, unshocked, and shocked gas, respectively.

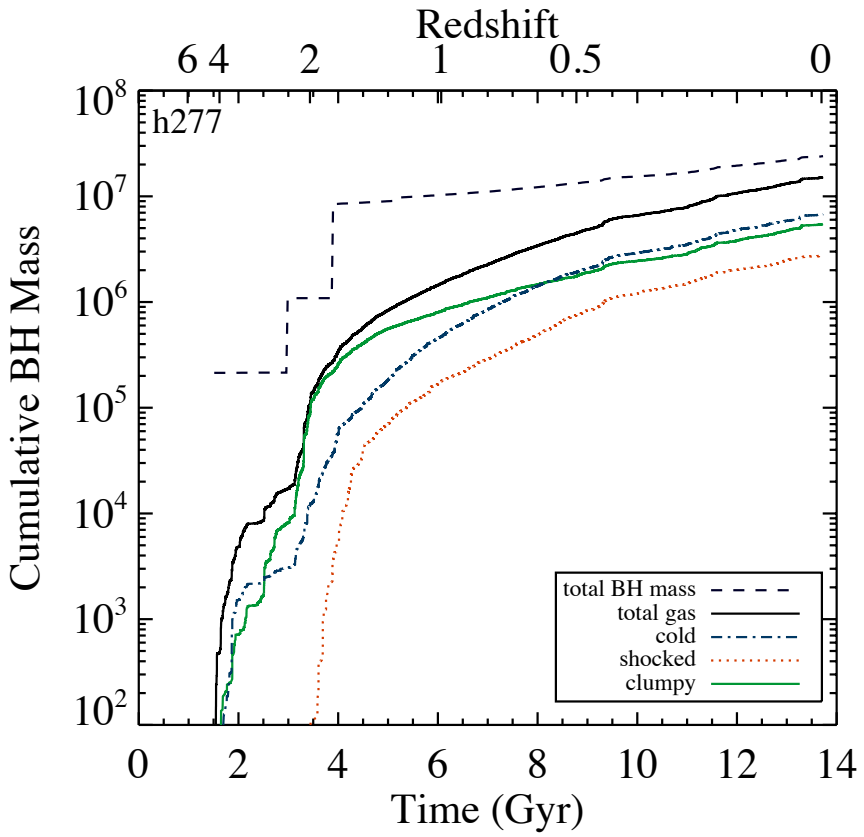

Fig. 8.— The central BHs cumulative mass as a function of time and redshift. The black dashed line indicates the total cumulative BH mass. The black solid line indicates the total gas mass. The blue dot-dashed line indicates the gas mass accreted via unshocked gas. The green solid line indicates the gas mass accreted through mergers. The red dashed line indicates gas mass that was shocked upon entry into the halo.

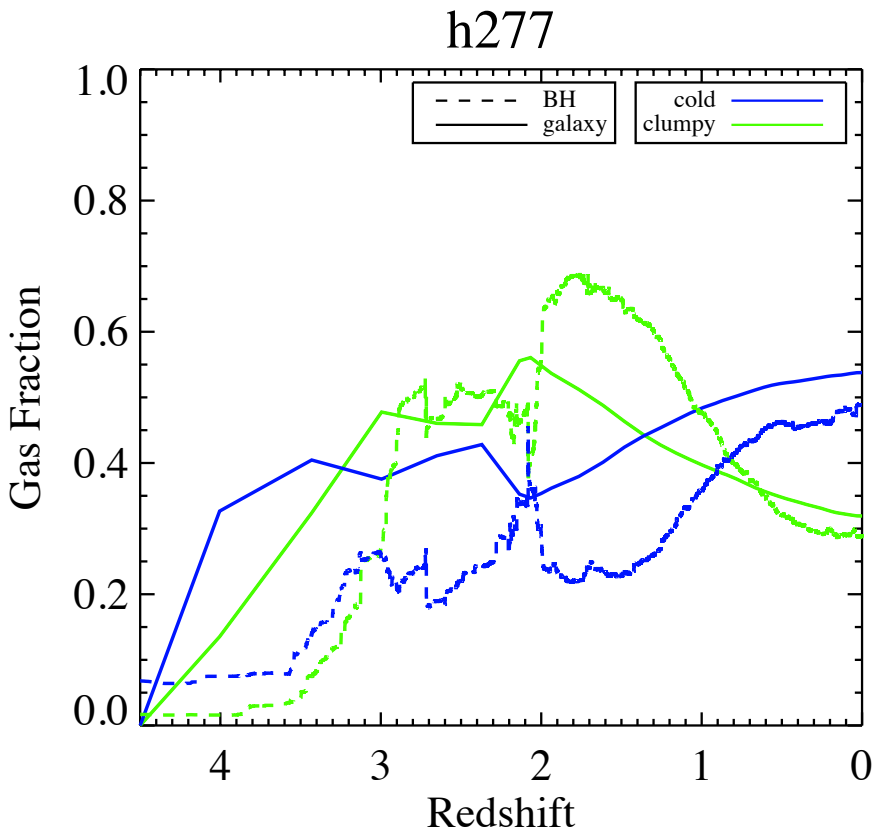

Fig. 9.— Gas fraction across redshift for galaxy (solid lines) and central BH (dashed lines). Green lines signify gas fractions accreted via mergers and blue lines designate gas accreted via unshocked gas filaments.

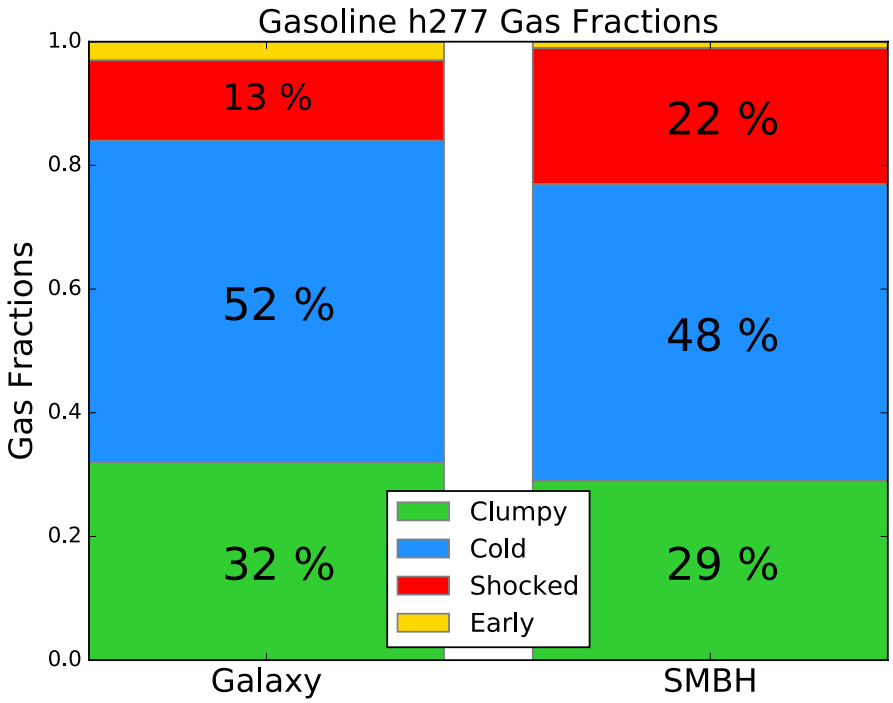

Fig. 10.— Gas fractions of the gas particles accreted in h258 by the main halo (left) and the SMBH (right), distinguished by type. Blue, green, and red distinguish gas gained through unshocked gas, gained through mergers, and gas shocked upon entry, respectively. Yellow indicates gas that existed within the main halo upon formation; this "early" gas is negligable (< 1 %) within the SMBH.

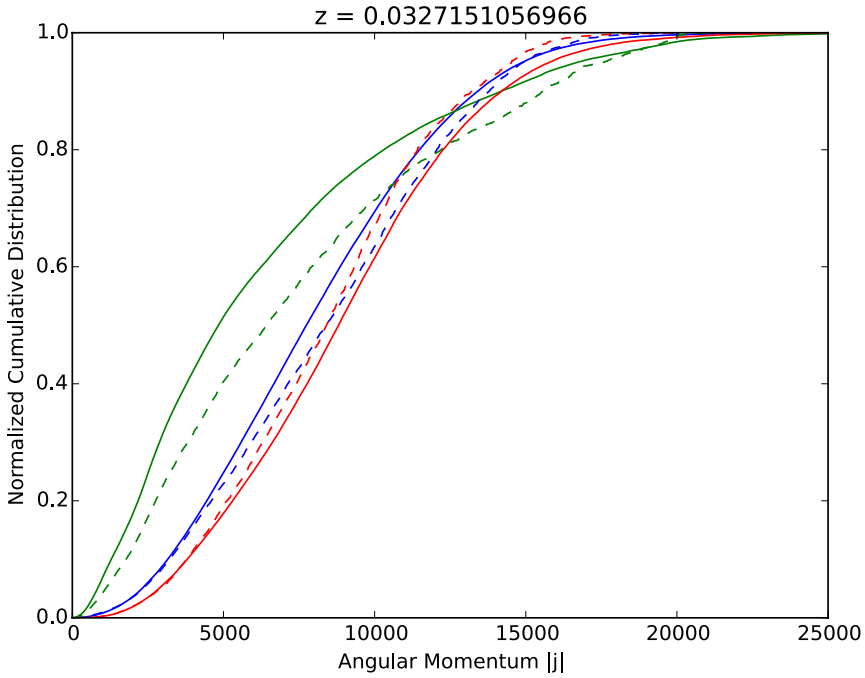

Fig. 11.— Cumulative distribution of angular momentum of the gas particles accreted onto h277. Gas particles accreted onto the main halo (solid lines) and central black hole (dashed lines). The green, blue, and red lines indicate clumpy, unshocked, and shocked gas, respectively.

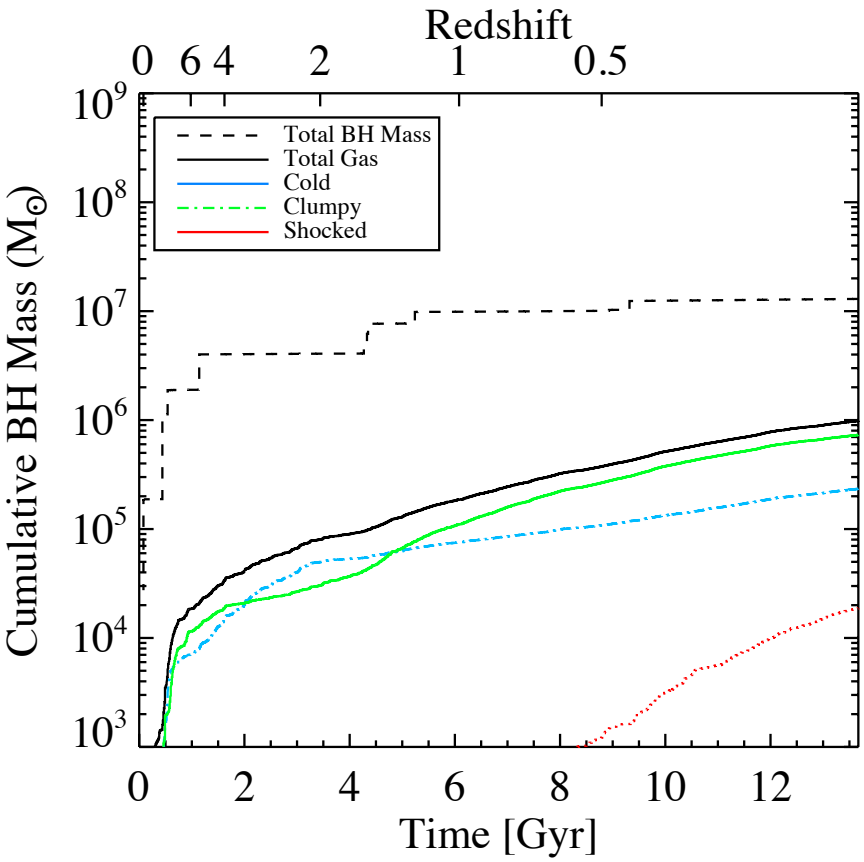

Fig. 12.— The central BHs cumulative mass as a function of time and redshift. The black dashed line indicates the total cumulative BH mass. The black solid line indicates the total gas mass. The blue dot-dashed line indicates the gas mass accreted via unshocked gas. The green solid line indicates the gas mass accreted through mergers. The red dashed line indicates gas mass that was shocked upon entry into the halo.

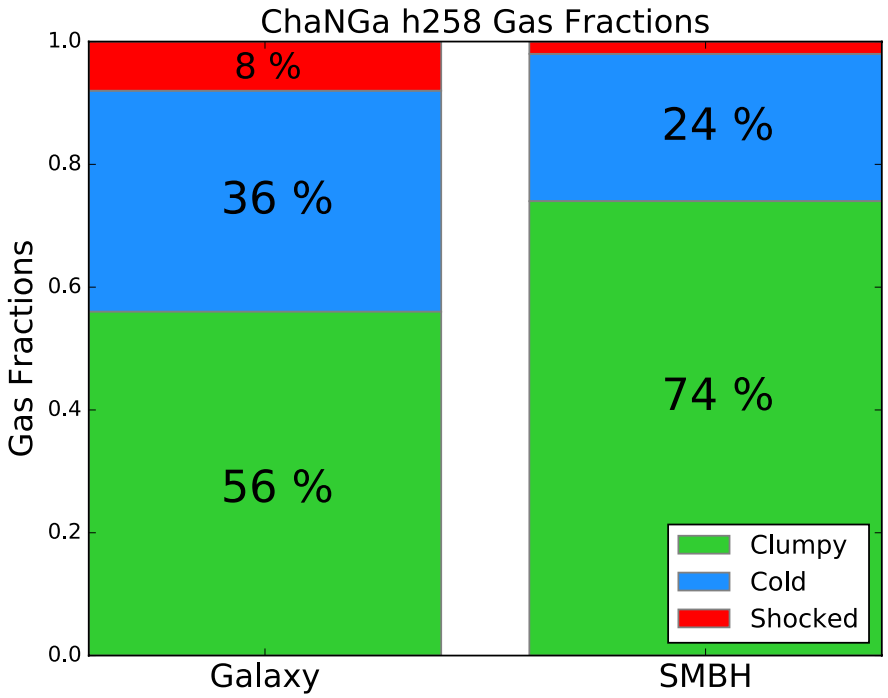

Fig. 13.— Gas fractions of the gas particles accreted by the high resolution ChaNGA h258 by the main halo (left) and the SMBH (right), distinguished by type. Blue, green, and red distinguish gas gained through unshocked gas, gained through mergers, and gas shocked upon entry, respectively. Yellow indicates gas that existed within the main halo upon formation; this "early" gas is negligable (< 1 %) within the SMBH.

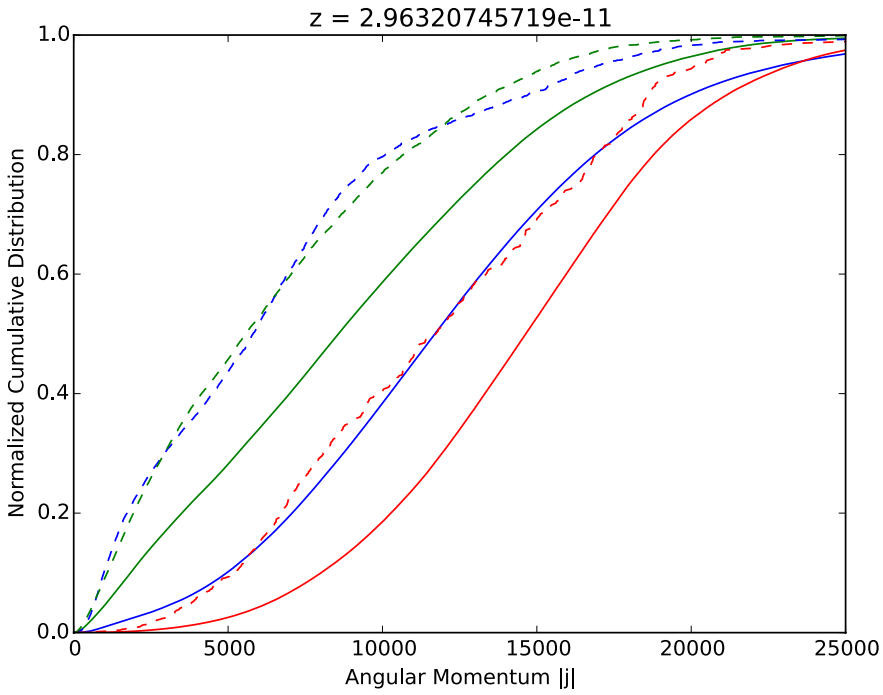

Fig. 14.— Cumulative distribution of angular momentum of the gas particles accreted onto the high resolution ChaNGa h258. Gas particles accreted onto the main halo (solid lines) and central black hole (dashed lines). The green, blue, and red lines indicate clumpy, unshocked, and shocked gas, respectively.

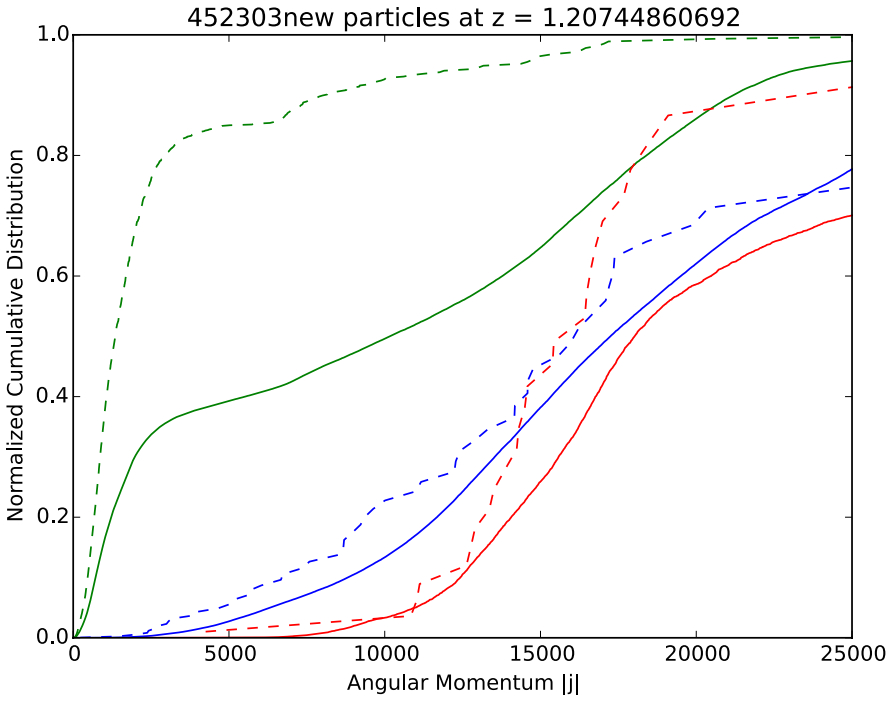

Fig. 15.— Cumulative distribution of angular momentum of the gas particles accreted onto the high resolution ChaNGA h258 galaxy at the time of the second major merger (z $\sim$ 1.2). There are about 450,000 gas particles accreted at this timestep, which gas particles accreted onto the main halo and central black hole are distinguished by solid and dashed lines. The green, blue, and red lines indicate clumpy, unshocked, and shocked gas, respectively.

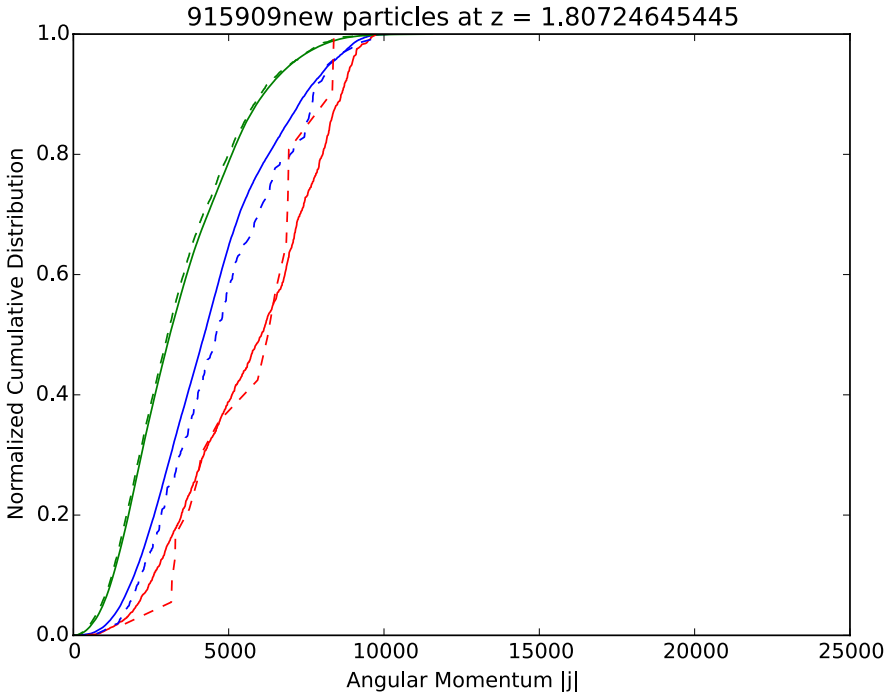

Fig. 16.— Cumulative distribution of angular momentum of the gas particles accreted onto the high resolution ChaNGA h258 galaxy at the time of the first major merger (z $\sim$ 1.8). There are about 900,000 gas particles accreted at this timestep, which gas particles accreted onto the main halo and central black hole are distinguished by solid and dashed lines. The green, blue, and red lines indicate clumpy, unshocked, and shocked gas, respectively.

REFERENCES

Abel, T. 2002, Science, 295, 93 2

Alexander, D. M., Smail, I., Bauer, F. E., et al. 2005, Nature, 434, 738 1

Alongi, M., Bertelli, G., Bressan, a., et al. 1993, Astronomy and Astrophysics Supplement Series, 97, 851 2

Begelman, M. C., Volonteri, M., & Rees, M. J. 2006, Monthly Notices of the Royal Astronomical Society, 370, 289 2

Bellovary, J., Brooks, A., Volonteri, M., et al. 2013, The Astrophysical Journal, 779, 136 1, 3, 4.1, 4.2, 5

Bellovary, J., Volonteri, M., Governato, F., et al. 2011, The Astrophysical Journal, 742, 13 2

Bertelli, G., Bressan, a., Chiosi, C., Fagotto, F., & Nasi, E. 1994, Astronomy and Astrophysics Supplement Series, 106, 275 2

Bressan, A., Fagotto, F., Bertelli, G., & Chiosi, C. 1993, Astronomy and Astrophysics Supplement Series (ISSN 0365-0138), 100, 647 2

Bromm, V., Ferrara, A., Coppi, P. S., & Larson, R. B. 2001, Monthly Notices of the Royal Astronomical Society, 328, 969 2

Bromm, V., & Larson, R. 2004, \Araa, 42, 79 2

Brooks, A. M., Governato, F., Booth, C. M., et al. 2007, The Astrophysical Journal, 655, L17 1, 2

Brooks, A. M., Governato, F., Quinn, T., Brook, C. B., & Wadsley, J. 2009, The Astrophysical Journal, 694, 396 3

Brooks, A. M., Solomon, A. R., Governato, F., et al. 2011, The Astrophysical Journal, 728, 51 2

Couchman, H. M. P., & Rees, M. J. 1986, Monthly Notices of the Royal Astronomical Society, 221, 53 2

Cox, T. J., Dutta, S. N., Di Matteo, T., et al. 2006, The Astrophysical Journal, 650, 791 1

Dekel, a., Birnboim, Y., Engel, G., et al. 2009, Nature, 457, 451 1

Di Matteo, T., Colberg, J., Springel, V., et al. 2008, \Apj, 676, 33 2

Di Matteo, T., Springel, V., & Hernquist, L. E. 2005, Nature, 433, 604 1

Dressler, A., & Richstone, D. O. 1988, The Astrophysical Journal, 324, 701 1

Eisenstein, D. J., & Loeb, A. 1995, The Astrophysical Journal, 443, 11 2

Ellison, S. L., Mendel, J. T., Patton, D. R., & Scudder, J. M. 2013, Monthly Notices of the Royal Astronomical Society, 435, 3627 1

Ferrarese, L., & Merritt, D. 2000, The Astrophysical Journal, 539, L9 1

Fu, H., & Stockton, A. 2008, 19 1

Gill, S. P. D., Kneb, A., & Gibson, B. K. 2004, Monthly Notices of the Royal Astronomical Society, 351, 399 3

Governato, F., Brook, C., Mayer, L., et al. 2009a, Nature, 463, 203 1, 2

Governato, F., Brook, C. B., Brooks, A. M., et al. 2009b, Monthly Notices of the Royal Astronomical Society, 398, 312 1, 2, 2.1

Graham, A. W., Onken, C. A., Athanassoula, E., & Combes, F. 2011, Monthly Notices of the Royal Astronomical Society, 412, 2211 1

Graham, A. W., & Scott, N. 2014, The Astrophysical Journal, 798, 54 1

Guedes, J., Callegari, S., Madau, P., & Mayer, L. 2011, The Astrophysical Journal, 742, 76 2

Haardt, F., & Madau, P. 2012, The Astrophysical Journal, 746, 125 2.2

Haehnelt, M. G., & Kauffmann, G. 2000, Monthly Notices of the Royal Astronomical Society, 318, L35 1

Hicks, E. K. S., Davies, R. I., Maciejewski, W., et al. 2013, The Astrophysical Journal, 768, 107 1

Holley-Bockelmann, K., Micic, M., Sigurdsson, S., & Rubbo, L. J. 2010, The Astrophysical Journal, 713, 1016 4.1

Hopkins, P. F., Hernquist, L., Cox, T. J., et al. 2006, The Astrophysical Journal Supplement Series, 163, 1 1

Hopkins, P. F., & Quataert, E. 2010, Monthly Notices of the Royal Astronomical Society, 407, 1529 1

Katz, N., & White, S. D. M. 1993, The Astrophysical Journal, 412, 455 2

Keller, B. W., Wadsley, J., Benincasa, S. M., & Couchman, H. M. P. 2014, Monthly Notices of the Royal Astronomical Society, 442, 3013 2.2

Keres, D., Katz, N., Weinberg, D. H., & David, R. 2005, Monthly Notices of the Royal Astronomical Society, 363, 2 1

Knebe, A., Green, A., & Binney, J. 2001, Monthly Notices of the Royal Astronomical Society, 325, 845 3

Knollmann, S. R., & Knebe, A. 2009, The Astrophysical Journal Supplement Series, 182, 608 3

Kocevski, D. D., Faber, S. M., Mozena, M., et al. 2011, 148, 10 1

Kormendy, J. 1993 1

Kormendy, J., & Ho, L. C. 2013, Annual Review of Astronomy and Astrophysics, 51, 511 1

Koushiappas, S. M., Bullock, J. S., & Dekel, A. 2004, Monthly Notices of the Royal Astronomical Society, 354, 292 2

Kroupa, P. 2001, \Mnras, 322, 231 2

Lodato, G., & Natarajan, P. 2006, Monthly Notices of the Royal Astronomical Society, 371, 1813 2

Loeb, A., & Rasio, F. A. 1994, PhD Proposal, 1, arXiv:9401026 2

Maiolino, R., Nagao, T., Grazian, A., et al. 2008, Astronomy and Astrophysics, 488, 463 2

Marconi, A., & Hunt, L. K. 2003, 21 1

Mcconnell, N. J., & Ma, C.-P. 2013, The Astrophysical Journal, 764, 184 1

McLure, R. J., & Dunlop, J. S. 2001, Journal of Chemical Information and Modeling, 53, 1689 1

Merritt, D., & Ferrarese, L. 2001a, Journal of Chemical Information and Modeling, 53, 1689 1

—. 2001b, The Astrophysical Journal, 547, 140 1

Micic, M., Holley-Bockelmann, K., Sigurdsson, S., & Abel, T. 2007, Monthly Notices of the Royal Astronomical Society, 380, 1533 1

Moster, B. P., Somerville, R. S., Maulbetsch, C., et al. 2010, The Astrophysical Journal, 710, 903 1, 2

Mullaney, J. R., Pannella, M., Daddi, E., et al. 2012, Monthly Notices of the Royal Astronomical Society, 419, 95 1

Munshi, F., Governato, F., Brooks, A. M., et al. 2013, The Astrophysical Journal, 766, 56 2

Natarajan, P. 2011, Bulletin of the Astronomical Society of India, 39, 145 1

Nelson, D., Vogelsberger, M., Genel, S., et al. 2013, Monthly Notices of the Royal Astronomical Society, 429, 3353 1

Ostriker, J. P., & McKee, C. F. 1988, Reviews of Modern Physics, 60, 1 2

Papovich, C., Moustakas, L. A., Dickinson, M., et al. 2006, The Astrophysical Journal, 640, 92 1

Raiteri, C. M., Villata, M., & Navarro, J. F. 1996, Astronomy and Astrophysics 2

Reddy, N. A., Steidel, C. C., Pettini, M., et al. 2008, The Astrophysical Journal Supplement Series, 175, 48 1

Reines, A. E., Greene, J. E., & Geha, M. 2013, \Apj, 775, 116 1

Richards, G. T., Strauss, M. a., Fan, X., et al. 2006, The Astronomical Journal, 131, 2766 1

Ritchie, B. W., & Thomas, P. A. 2001, 756 2.2

Ryan, C. J., De Robertis, M. M., Virani, S., Laor, A., & Dawson, P. C. 2007, The Astrophysical Journal, 654, 799 1

Schawinski, K., Treister, E., Urry, C. M., et al. 2011, The Astrophysical Journal, 727, L31 1

Shen, J., Vanden Berk, D. E., Schneider, D. P., & Hall, P. B. 2008, The Astronomical Journal, 135, 928 1

Sijacki, D., Springel, V., Di Matteo, T., & Hernquist, L. 2007, Monthly Notices of the Royal Astronomical Society, 380, 877 2

Sijacki, D., Springel, V., & Haehnelt, M. G. 2009, Monthly Notices of the Royal Astronomical Society, 400, 100 1

Silverman, J. D., Lamareille, F., Maier, C., et al. 2009, The Astrophysical Journal, 696, 396 1

Sinha, M., & Holley-Bockelmann, K. 2012, The Astrophysical Journal, 751, 17 1

Spergel, D. N., Bean, R., Dore, O., et al. 2007, 288 2

Springel, V., & Hernquist, L. 2005, The Astrophysical Journal, 622, L9 1

Stinson, G., Seth, A., Katz, N., et al. 2006, Monthly Notices of the Royal Astronomical Society, 373, 1074 2

Thielemann, F.-K., Nomoto, K., & Yokoi, K. 1986, Astronomy and Astrophysics (ISSN 0004-6361), 158, 17 2

Treister, E., Schawinski, K., Urry, C. M., & Simmons, B. D. 2012, The Astrophysical Journal, 758, L39 1

Van Den Bosch, F. C., Yang, X., Mo, H. J., et al. 2007, Monthly Notices of the Royal Astronomical Society, 376, 841 1

van Gorkom, J., & Schiminovich, D. 1997, ASP Conference Series, 116, 310 1

Volonteri, M. 2012, Science, 337, 544 1

Volonteri, M., Lodato, G., & Natarajan, P. 2008, Monthly Notices of the Royal Astronomical Society, 383, 1079 2

Volonteri, M., & Natarajan, P. 2009, Monthly Notices of the Royal Astronomical Society, 400, 1911 1

Wadsley, J., Stadel, J., & Quinn, T. 2003, New Astronomy, 9, 137 2, 2.1

Woosley, S. E., & Weaver, T. A. 1986, Annual Review of Astronomy and Astrophysics, 24, 205 2